Ecological Indicators 143 (2022) 109410

Contents lists available at ScienceDirect

Ecological Indicators

journal homepage: www.elsevier.com/locate/ecolind

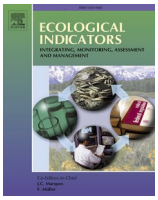

Original Articles

An integrated approach for identification and quantification of ecological drought in rivers from an ecological streamflow perspective

Shanhu Jiang [a,b], Menghao Wang [a,b,*], Liliang Ren [a,b,*], Yating Liu [b], Le Zhou [b], Hao Cui [b], Chong-Yu Xu [c]

[a] State Key Laboratory of Hydrology-Water Resources and Hydraulic Engineering, Hohai University, Nanjing 210098, China
[b] College of Hydrology and Water Resources, Hohai University, Nanjing 210098, China
[c] Department of Geosciences, University of Oslo, Oslo, Norway

ARTICLE INFO

Keywords:
Ecological streamflow
Variable threshold method
Ecological drought
Climate change
Human activities

ABSTRACT

Although various studies have investigated the impacts of climate variability and human activities on drought, researches specifically analysing the impact on ecological drought are still limited. A deep understanding of the climatic and anthropogenic effects on ecological drought processes is crucial for ecological regulation and management in the changing environments. In the present study, an integrated approach for comprehensive understanding and quantification of ecological drought in rivers was proposed which first applied the nonparametric kernel density estimation (KDE) method to calculate the most suitable ecological streamflow (MSES) for a river ecosystem. Then, the variable threshold level method based on the MSES for each month and the run theory method were applied to identify the ecological drought duration and deficit volumes. Finally, a quantification approach based on hydrological model simulation was proposed to attribute the impacts of climate variability and human activities on ecological drought. The proposed approach was applied on two catchments, Xianyang (XY) and Huaxian (HX) within the Weihe River Basin (WRB) in northern China. Comparison results obtained using the two empirical methods revealed that the MSES calculated using the KDE method was reasonable and can be used for ecological drought identification. The identification results showed that both the median and upper quartile values of the drought duration and deficit volumes during the disturbed period (1991–2017) were greater than those during the undisturbed period (1961–1990). Quantification results showed that human activities were the dominant factor aggravating ecological drought in the WRB after 1990. The contribution rates of climate variability and human activities toward ecological drought variations were 25.6% and 74.4%, respectively, for the XY station and 42.7% and 57.3%, respectively, for the HX station. Although the WRB was selected as a case study, the proposed approach can also be applied to other regions to provide scientific guidance for regional ecological management.

1. Introduction

Drought is one of the most widespread and serious natural disasters around the world, which poses a serious threat to food security, water supply security and ecological security (Van Loon et al., 2016; Jiang et al., 2019, 2021a; Vicente-Serrano et al., 2020; Wang et al., 2020, 2021a; Zhou and Zhou, 2021; Ma et al., 2022). Considering the difficulty of drought research and practical application, drought is usually divided into different types, namely meteorological drought, agricultural drought, hydrological drought, and socioeconomic drought (Eltahir and Yeh, 1999; Peters et al., 2003; Mishra and Singh, 2010; Apurv and Cai, 2020). However, Crausbay et al. (2017) noted that the existing definitions and classifications of drought describe meteorological drought impacts through a human-centric lens and ecosystem responses to drought tend to be ignored. Meanwhile, global climate change and various anthropogenic activities have increased the vulnerability of ecosystems to drought, which can considerably affect the service capacity of ecosystems to human society (Tonkin et al., 2019). Thus, it is imperative to recognise ecological drought processes to maintain ecosystems and provide sustainable services to human communities

* Corresponding authors at: State Key Laboratory of Hydrology-Water Resources and Hydraulic Engineering, Hohai University, Nanjing 210098, China (Menghao Wang & Liliang Ren).
E-mail addresses: mhwang@hhu.edu.cn (M. Wang), njrll9999@126.com (L. Ren).

https://doi.org/10.1016/j.ecolind.2022.109410
Received 11 July 2022; Received in revised form 29 August 2022; Accepted 31 August 2022

(Vicente-Serrano et al., 2020).

Recently, there have been some studies focus on ecological drought from the perspective of terrestrial ecosystems (Hasanuzzaman et al., 2019; Kim et al., 2019; Park et al., 2020; Jiang et al., 2021c; Bilen and Turan, 2022). Remote sensing technology plays a significant role in monitoring ecological droughts in terrestrial ecosystems. A vegetation index based on remote sensing can indirectly reflect the changes in terrestrial ecosystems under drought conditions and is a useful tool to characterise vegetation droughts (Carlson et al., 1994; Roodposhti et al., 2017; Nanzad et al., 2019; Measho et al., 2019; Yan et al., 2019, Hasanuzzaman et al., 2019). In addition, the streamflow regime has long been known to be a key factor in the health of aquatic ecosystems, thus providing valuable information for monitoring ecological drought in aquatic ecosystems (McEvoy et al., 2018; Palmer and Ruhi, 2019; Park et al., 2020; Jiang et al., 2021b; McMillan, 2021). For example, McEvoy et al. (2018) utilised a new ecological drought framework based on ecological streamflow to analyse drought plans of southwestern Montana, USA. Park et al. (2020) analysed the ecological flow regimes of a river with double thresholds to develop an ecological drought index for fish habitats to assess ecological droughts processes during extremely low flow regimes. Thus, based on the definition of ecological drought proposed by Crausbay et al. (2017), this study adopted ecological streamflow as a threshold to determine whether a river ecosystem is in an ecological drought condition.

To date, major efforts have been made to define or calculate ecological streamflow according to the eco-hydrological relationship (Richter et al., 2006; Jiang et al., 2021c). Currently, there are four types of method, including the hydrological, hydraulic rating, habitat simulation, and holistic methods (Tharme 2003). However, the hydraulic rating, habitat simulation, and holistic methods require a lot of support data (McManamay et al., 2013; Pastor et al., 2014) or are time-consuming (Poff et al., 2010; Shafroth et al., 2010). The hydrological methods are proposed earlier than the above three methods and have been more developed so far. Meanwhile, hydrological analysis is a basic and effective method for the preliminary study of river ecological streamflow processes, when other ecological datasets are not available. The current hydrological methods for calculating ecological flow are typically based on grading standards and lack a unified definition and standard (Ma et al., 2019). For example, two widely used methods, the Tennant (Tennant, 1976) and Smakhtin (Smakhtin et al., 2004) methods, which primarily use a specific guarantee rate, usually have deviations due to the annual distribution inequality or some extreme events (Ma et al., 2019). Therefore, based on the bio-adaptability (Wilson and Franklin, 2002) and plasticity theory (Ow et al., 2010) of an ecosystem, this study introduced the concept of the most suitable ecological streamflow (MSES) proposed by Ma et al. (2019) to select the monthly river streamflow corresponding to the maximum probability density as the MSES for that month, and then combined the MSES of each month to compose a monthly variable threshold for the identification of ecological drought in rivers.

It is worth noting that under global change, the driving forces for the evolution of ecological drought have gradually transitioned from a single natural factor, i.e., climate variability to a combination of "natural-human" factors, i.e., climate variability and human activities" (Van Loon et al., 2016; Akcura et al., 2019; Ghasempour et al., 2022). In addition to traditional climate variability, the hydraulic engineering regulations and anthropogenic water use behaviours may also alter natural river regimes, and then influence the propagation of ecological drought in rivers (Park et al., 2020; Gudmundsson et al., 2021; Tauqeer et al., 2022; Wang et al., 2022). However, there are limited studies on how to define and calculate the most suitable ecological streamflow, how to identify ecological drought in rivers, and how climate variability and anthropogenic activities alter ecological drought in rivers processes. A deep understanding of these problems is critical for ecological management and regulation in the Anthropocene era.

To overcome the above-mentioned limitations, this study proposes an approach for identifying and quantifying ecological drought in rivers from the perspective of ecological streamflow. The approach includes four parts: (1) identifying a change point to divide the entire study period into two parts, i.e., undisturbed and disturbed periods before and after the change point; Using hydro-meteorological data in undisturbed period to calibrate a hydrological model, and then simulating the natural streamflow processes in the disturbed period; (2) using the nonparametric kernel density estimation (KDE) method (Bowman and Azzalini, 1997; Kim et al., 2019) to calculate the MSES based on the observed streamflow series during the undisturbed periods; (3) using the calculated monthly MSES series to compose a monthly variable threshold series and combining it with the run theory to identify ecological drought events and corresponding drought duration and deficit volumes; and (4) proposing a quantification approach to compare ecological drought characteristics of different series in different periods to quantify the influence of climate variability and human activities on ecological drought. In this study, we selected the Weihe River Basin (WRB) in northern China as the study area because the basin is highly affected by human beings. This study will enrich the discipline of ecological hydrology and provide scientific guidance for regional ecological management.

2. Study area and data

2.1. Study area

The WRB, located in the northern China, is the largest tributary basin of the Yellow River Basin. In the present study, we focused on the WRB above the Huaxian station (Fig. 1), which covers a drainage area of 106,000 km^2 and extends from 104 °E to 110 °E and from 33 °N to 38 °N. The elevation within the study area ranges from 326 to 3733 m with a significant decrease from northwest to southeast. We selected the Xianyang (XY) and Huaxian (HX) stations (as shown in Fig. 1) as case studies to analyse ecological drought. Because WRB is situated in a continental monsoon climate zone, the study area experiences rich precipitation and high temperature in summer but sparse precipitation and low temperature in winter (Huang et al., 2017). The average annual precipitation (1961–2017) of the study area is 584.4 mm and its precipitation has a noticeable seasonality, with more than 65 % of annual precipitation occurring in flood season (from June to September). The average annual temperature (1961–2017) of the study area reaches 7.7 ℃. The mean air temperature in the coldest month (January) ranges from –8.8 ℃ to –2.4 ℃, whereas that in the hottest month (July) varies from 18.9 ℃ to 23.2 ℃. The average annual streamflow for the XY and HX stations during 1961–2017 are 78.2 and 59.7 mm, respectively.

The quality of WRB's river ecology directly affects the quality of the ecology in the middle reaches of the Yellow River Basin. Several studies have pointed out that with rapid socio-economic development, human water abstraction activities, such as domestic and industrial water requirements and agricultural irrigation, have a profound impact on the streamflow of the WRB (Xiong et al., 2014, Gai et al., 2019), resulting in increasingly serious ecological drought problems in rivers of the basin (Ren et al., 2016; Huang et al., 2017; Zou et al., 2018; Gai et al., 2019; Fang et al., 2020; Zhang et al., 2021).

2.2. Data

The observed daily precipitation data of 62 rain gauge stations and the streamflow data from the two hydrological stations between 1961 and 2017 were obtained from the Hydrological Bureau of the Ministry of Water Resources of China. Meteorological data, including maximum and minimum temperatures and wind speeds from 26 meteorological stations, were provided by the China Meteorological Administration (CMA). The daily precipitation and meteorological data were converted into spatially distributed grid data (0.25° × 0.25°) using the inverse distance weighting interpolation method to drive a distributed

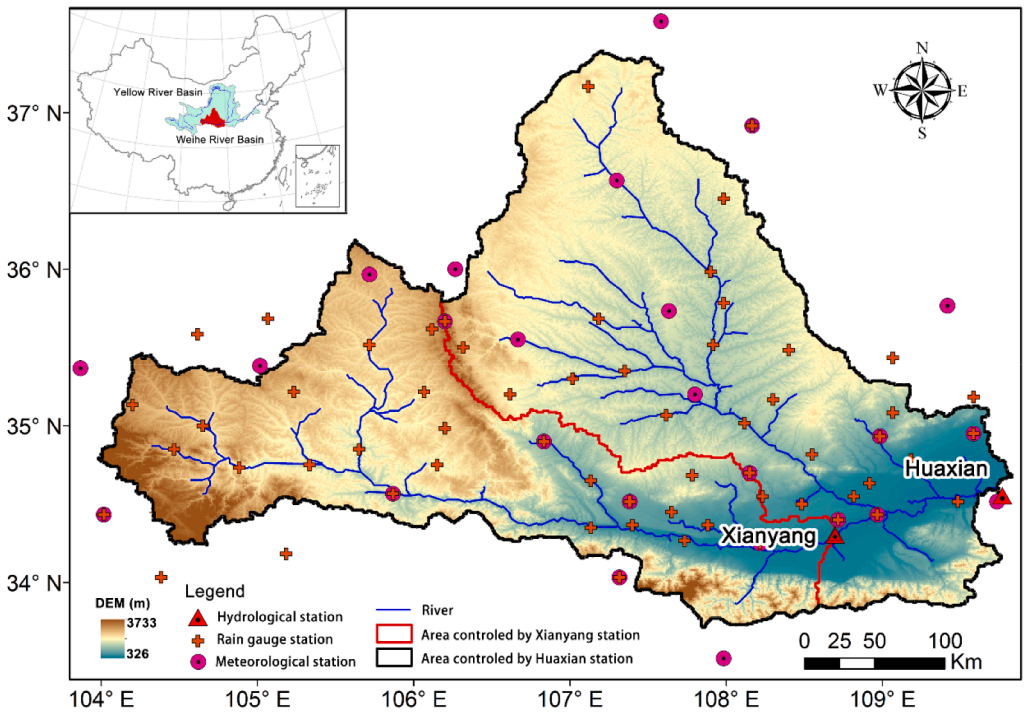

Fig. 1. Location of the study area and distribution of the rain gauge, meteorological, and hydrological stations within the Weihe River Basin (WRB).

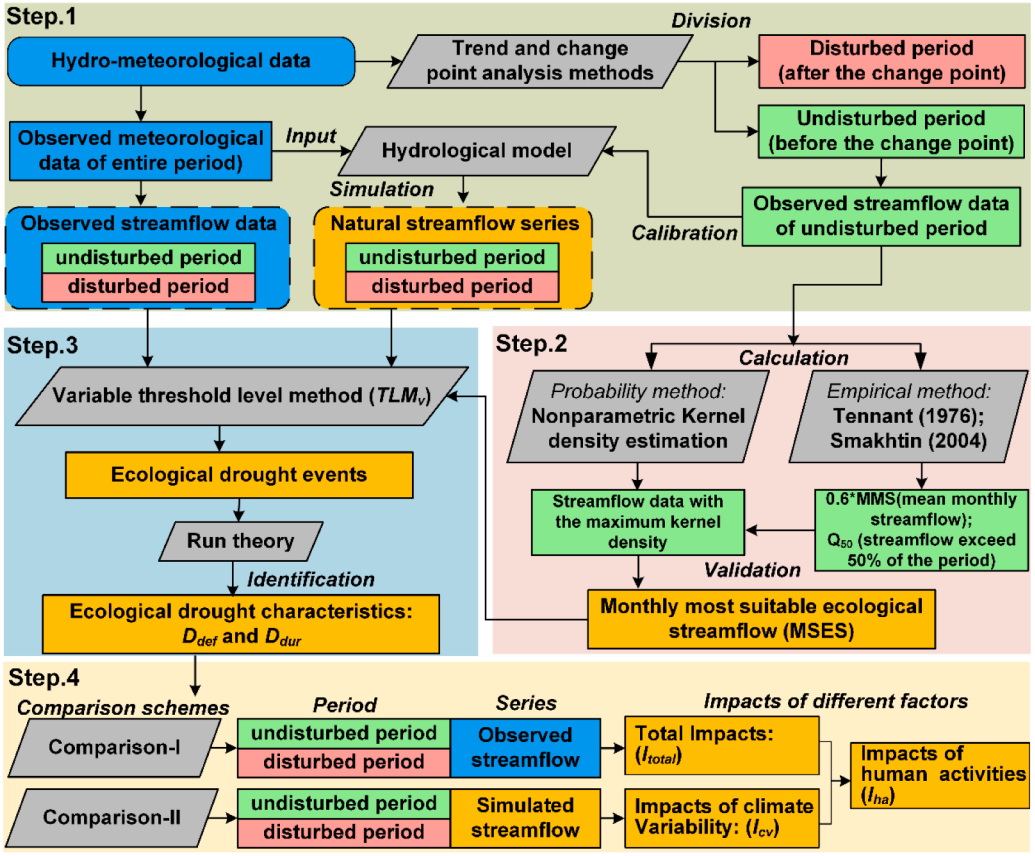

Fig. 2. Flow chart of identification and quantification of the impacts of climate variability and human activities on ecological drought.

hydrological model.

3. Methods

As shown in Fig. 2, the flow chart of the proposed an approach comprises four main steps. The first step is the reconstruction of natural streamflow. Regarding to the analysis results of the trend and change point of the streamflow series, the entire study period can be divided into two periods, the undisturbed period with weak interference from human activities, and the disturbed period with strong influence from human activities (Van Loon and Van Lanen, 2013). Next, the variable infiltration capacity (VIC) model was first calibrated using the observed meteorological and streamflow data from the undisturbed period, and then the calibrated model (with parameters remaining unchanged) was used to simulate the streamflow series during the disturbed period with the observed meteorological forcing data in the same period as the input data. In the second step, the nonparametric KDE probability method was adopted to calculate the MSES based on the observed streamflow series during the undisturbed period. Meanwhile, two widely used empirical methods, the Tennant (Tennant, 1976) and Smakhtin (Smakhtin et al., 2004) methods, were selected to validate the rationality of the MSES calculated according to the KDE method. In the third step, the calculated monthly MSES series was used to compose a variable threshold series and combine it with the run theory to identify the ecological drought events and their characteristics, including the drought duration (D_{dur}) and deficit volumes (D_{def}) of different series (i.e., simulated and observed series) during different periods (i.e., disturbed and undisturbed periods). In the final step, two comparisons were carried out to separate the impacts of climatic and anthropogenic influences—comparison I was performed to identify the total influence of climate variability and human activities using the ecological drought of the observed streamflow values during the undisturbed and disturbed periods, and the purpose of comparison II was to identify the impacts of only climate variability using the ecological drought of simulated streamflow during the undisturbed and disturbed periods. The total influence minus the impact of climate variability provided the anthropogenic influence. The detail information of methods and concepts used in this study are described as below.

3.1. Trend and change point analysis methods

3.1.1. Trend analysis methods

The Modified Mann-Kendall (MMK) test method, proposed by Hamed and Rao (1998), uses the *lag-i* autocorrelation to remove the persistence of the hydrometeorological series to improve the original Mann-Kendall test method to make the results more reliable and robust. In this method, the value of the test statistic (*Z-values*) is used to determine the upward and downward trends. $Z > 1.96$ and $Z < -1.96$ correspond to significant upward and downward trends, respectively, at the 5 % significance level. More detailed information of the MMK method can refer to Hamed and Rao (1998).

3.1.2. Change point analysis methods

Conventional statistical test methods for identification of change points such as Mann-Kendell test and sliding *T* test are usually based on the assumption that the time series should be linear and stationary. However, it is difficult for them to accurately capture the change points in the nonlinear or nonstationary time series. To make up this shortcoming, this study applied the heuristic segmentation method, proposed by Bernaola-Galvan et al. (2001), to identify change points in nonlinear and nonstationary series. Firstly, this method divides a time series into two subseries by a point, and the averages of the two subseries are calculated. Then, by moving the point along the given time series in a stepwise fashion, the *t*-statistic can be calculated to assess the differences between the averages of the two sub-series. The location resulting in the largest *t*-value (t_{max}) can then be considered as a change point. When the statistical significance of t_{max} (i.e., $P(t_{max})$) is higher than the selected threshold (we selected the 95 % significance level in the present study), the corresponding point is defined as a change point, and then the time series is divided into two segments.

In addition, the double cumulative curve (DCC) method is another widely used method for identifying the change points. Generally, the inflection point of a curve of precipitation and streamflow can be selected as a change point.

3.2. VIC hydrological model

The VIC model is a macroscale semi-distributed hydrological model based on Soil-Vegetation-Atmospheric Transfer Schemes (SVATS) and has a widely application worldwide (Liang et al., 1994). The VIC model divides the soil column of each grid cell into three layers (Gou et al., 2020), and the surface flow generated from the upper two soil layers is simulated based on the variable soil moisture capacity curve, which is expressed as:

$$W = W_{mm}\left(1 - (1 - A)^{1/B}\right) \tag{1}$$

where W and W_{mm} are the soil moisture capacity at a grid point and the maximum soil moisture capacity at that point, respectively; A is the fraction of area within the grid cell for which the soil moisture capacity is less than W; and B is the soil moisture capacity shape parameter. The surface flow, Q_s, is calculated as:

$$Q_s = \begin{cases} PE - (W_m - W_0), & PE + W \geqslant W_{mm} \\ PE - (W_m - W_0) + W_{mm}\left(1 - \dfrac{PE + W}{W_{mm}}\right)^{1+B}, & PE + W < W_{mm} \end{cases} \tag{2}$$

where PE is effective precipitation, which equals precipitation minus evapotranspiration; W_m is soil moisture capacity of the upper two soil layers; and W_0 is initial soil moisture.

The slow response runoff or baseflow, is only generated from the third layer. Using the nonlinear ARNO model, baseflow, Q_b, is modeled as:

$$Q_b = \begin{cases} \dfrac{D_s D_m}{W_s \theta_{3,s}}\theta_3, & 0 \leqslant \theta_3 \leqslant W_s\theta_{3,s} \\ \dfrac{D_s D_m}{W_s \theta_{3,s}}\theta_3 + \left(D_m - \dfrac{D_s D_m}{W_s}\right)\left(\dfrac{\theta_3 - W_s\theta_{3,s}}{\theta_{3,s} - W_s\theta_{3,s}}\right)^2, & \theta_3 > W_s\theta_{3,s} \end{cases} \tag{3}$$

where D_m is the maximum velocity of baseflow, D_s and W_s are the fraction of D_m and maximum soil moisture content of the third soil layer ($\theta_{3,s}$), respectively; and θ_3 is the current soil moisture of the third layer. The baseflow recession curve is linear below a threshold ($W_s\theta_{3,\ s}$) and nonlinear above that threshold.

According to previous studies, the model parameters can be

Table 1
Physical meanings and numerical ranges of the seven parameters commonly calibrated in the VIC model and their optimized values in this study.

Parameter	Physical meaning/Unit	Range	Optimized values	
			XY	HX
B	Infiltration curve parameter	0–0.4	0.37	0.15
d_1	Thickness of top thin soil moisture layer (m)	0.05–0.1	0.1	0.1
d_2	Thickness of middle soil moisture layer (m)	0–2	0.6	0.7
d_3	Thickness of lower soil moisture layer (m)	0–2	2.0	2.0
D_s	Fraction of D_{smax} where nonlinear baseflow begins	0–1	0.004	0.004
D_{smax}	Maximum velocity of baseflow (mm/d)	0–30	10.0	10.0
W_s	Fraction of maximum soil moisture where nonlinear baseflow occurs	0–1	0.8	0.8

classified into two groups (Liang et al., 2004). The first group consists of parameters that have clear physical meanings and can be determined directly from land use data and soil type data, such as the saturated soil potential ψ_s (m), soil porosity θ_s (m^3/m^3), saturated hydraulic conductivity k_s (m/s), and so on. The second group consists of seven conceptual parameters that need to be calibrated. The details of these user-calibrated parameters are listed in Table 1.

3.3. Calibration and validation of VIC model

In this study, the year 1961 (1 year) was selected as a warm-up period for the VIC model. Then the model was calibrated and validated at the two stations (XY and HX stations) during 1962–1980 (19 years) and 1981–1990 (10 years), respectively. According to the previous studies (Jiang et al., 2011, Ren et al., 2016; Yuan et al., 2018), the Infiltration curve parameter (B) and thickness of middle soil moisture layer (d_2) are the most sensitive two parameters among the seven parameters listed in Table 1. Then the parameter optimization of the VIC model was performed using SCE-UA algorithm (Duan et al., 1992) with the function (f) that combines the maximum sum value of the Nash-Sutcliffe efficiency (NSE) and the maximum value of log-transformed *NSE* (*logNSE*) as an objective function.

$$f = max(0.5 \times NSE + 0.5 \times logNSE) \tag{4}$$

$$NSE = 1 - \frac{\sum_{i=1}^{n}(Q_{sim}(i) - Q_{obs}(i))^2}{\sum_{i=1}^{n}(Q_{obs}(i) - \bar{Q_{obs}})^2} \tag{5}$$

$$logNSE = 1 - \frac{\sum_{i=1}^{n}(logQ_{sim}(i) - logQ_{obs}(i))^2}{\sum_{i=1}^{n}(logQ_{obs}(i) - \bar{logQ_{obs}})^2} \tag{6}$$

where, $Q_{obs}(i)$ and $Q_{sim}(i)$ are the observed and simulated streamflow values (mm/month) at time step i, respectively; $logQ_{obs}(i)$ and $logQ_{sim}(i)$ denote the log-transformed observed and simulated streamflow;$\bar{Q_{obs}}$,$\bar{Q_{sim}}$, and $\bar{logQ_{obs}}$ are the mean values of observed, simulated, and log-transformed observed streamflow, respectively; n is the length of time series.

It is worth noting that although *NSE* (log*NSE*) is a good metric for hydrological model optimization, it tends to provide high importance to high (low) flows (Oudin et al., 2006). To make sure that the model can capture both high- and low-flow processes, we used the maximum sum of *NSE* and log*NSE* (*NSE* and log*NSE* have the same weight, i.e., 0.5) as the objective function (f in Equation (4)). Because low-flow process is closely related to the onset and development stage of drought, and high-flow process is often related to termination stage of drought.

Furthermore, the performance of the VIC model was evaluated using another two indicators, i.e., Kling-Gupta efficiency (*KGE*) and relative error (*BIAS*).

$$KGE = 1 - \sqrt{(1-\gamma)^2 + (1-\alpha)^2 + (1-\beta)^2}, \qquad \alpha = \sigma_s/\sigma_o, \qquad \beta = \mu_s/\mu_o \tag{7}$$

$$BIAS = \frac{\sum_{i=1}^{n}(Q_{sim}(i) - Q_{obs}(i))}{\sum_{i=1}^{n}Q_{obs}(i)} \tag{8}$$

where, μ_s and σ_s are the mean and standard deviation of the simulation series, respectively; μ_o and σ_o are the mean and standard deviation of the observation series, respectively; and γ is the correlation coefficient between observation and simulation series. The value of f and/or *KGE* ranges from negative infinity to 1. When f and/or *KGE* is equal to 1 and *BIAS* is equal to 0, it indicates perfect runoff simulations.

3.4. Calculation of the most suitable ecological flow

Two empirical methods proposed by Tennant (Tennant, 1976) and Smakhtin (Smakhtin et al., 2004) are widely used to determine the health conditions of river ecosystems. In the Tennant method, the optimum range of streamflow for a river ecosystem is 60–100 % of the mean annual or mean monthly streamflow. We selected 60 % of the mean monthly streamflow as the MSES for this method. In the Smakhtin method, the Q_{50} (where the streamflow exceeds 50 % of the period of record) is a measure for a natural river ecosystem; according to this method, to maintain an ecosystem in natural conditions, the monthly streamflow should not be less than Q_{50}. Therefore, we selected Q_{50} as the MSES for the Smakhtin method.

In addition, we applied the KDE function (Bowman and Azzalini, 1997) to estimate the probability density of the monthly streamflow series. The streamflow value corresponding to the maximum KDE was selected as the MSES for a specific month (January to December). Then, the MSES calculated using the two empirical methods was used to validate the MSES calculated with the KDE method.

KDE calculation steps are as follows:

For the streamflow series x_1, x_2, …, x_n, the KDE function can be defined as:

$$\hat{f_h}(x) = \frac{1}{nh}\sum_{i=1}^{n}K\left(\frac{x_i - x}{h}\right), \qquad x \in R \tag{9}$$

where $K(\bullet)$ is the kernel function, and h is the bandwidth. $K(\bullet)$ satisfies $K(x) > 0$ and the $\int_{-\infty}^{+\infty}K(x)dx = 1$. Common kernel functions include uniform (box), triangle, Epanechnikov, Triweight, and Gaussian functions. In this study, we adopted the Gaussian kernel function. When the Gaussian function is used, the optimal choice for the bandwidth (h) is expressed as:

$$h = \left(\frac{4}{3}\right)^{\frac{1}{5}}\sigma n^{\frac{1}{5}} \approx 1.06\sigma n^{\frac{1}{5}} \tag{10}$$

where σ is the standard deviation of the sample, and n is the number of samples.

3.5. Identification of ecological drought characteristics

In this study, the MSES calculated in section 3.3 was selected to define a monthly variable threshold level (*TL*) to determine whether the river ecosystem is in ecological drought. Then, ecological drought duration and deficit volume can be identified from the observed and simulated monthly streamflow series using the run theory (Yevjevich, 1967; Wanders and Wada, 2015). Here, the per-time-step drought state ($Ds(t)$) and deficit volume ($D_{def}(t)$) are given as follows:

$$\begin{aligned} Ds(t) &= 1, \quad \text{for} \quad Q(t) < TL \\ &= 0, \quad \text{for} \quad Q(t) \geqslant TL \end{aligned} \tag{11}$$

$$\begin{aligned} D_{def}(t) &= TL - Q(t), \quad \text{for} \quad Ds(t) = 1 \\ &= 0, \quad \text{for} \quad Ds(t) = 0 \end{aligned} \tag{12}$$

where $Ds(t)$ is a binary variable to reflect whether a drought occurs at a given time t, $D_{def}(t)$ and $Q(t)$ are the drought deficit volume and the

monthly streamflow at a given time t, and TL is the ecological threshold level that used to determine whether a drought event will occur. The drought duration (D_{dur}) and deficit volume (D_{def}) of the drought event i were calculated as follows:

$$D_{dur}(i) = \sum_{t=F_i}^{L_i} Ds(t) \tag{13}$$

$$D_{def}(i) = \sum_{t=F_i}^{L_i} D_{def}(t) \tag{14}$$

where $D_{dur}(i)$, $D_{def}(i)$, and F_i and L_i are the drought duration, total drought deficit volume, and the first- and last-time steps of the drought event i, respectively.

3.6. Attribution of the impacts of climate variability and human activities on ecological drought

The quantification approach was proposed according to the following two assumptions: (1) climate variability and human activities are the two main factors causing variations in ecological drought; (2) the effects of these two factors are independent of one another, i.e., the interaction between them is negligible. D_{def} was selected as the variable to separate the impacts of climate variability and human activities on ecological drought during the disturbance period (Ren et al., 2016). The changes in the D_{def} of the observed series during undisturbed and disturbed conditions (i.e., Comparison I in Fig. 2) are expressed as:

$$\Delta S_{total} = \Delta S_{cv} + \Delta S_{ha} = S_{2,obs} - S_{1,obs} \tag{15}$$

The changes in D_{def} caused by climate variability (i.e., Comparison II in Fig. 2) can be expressed as follows:

$$\Delta S_{cv} = S_{2,sim} - S_{1,sim} \tag{16}$$

Furthermore, the changes in D_{def} caused by human activities can be expressed as follows:

$$\Delta S_{ha} = \Delta S_{total} - \Delta S_{cv} = (S_{2,obs} - S_{1,obs}) - (S_{2,sim} - S_{1,sim}) \tag{17}$$

Together, the effects of climate variability and human activities on ecological D_{def} can be calculated as follows:

$$I_{cv} = \frac{\Delta S_{cv}}{|\Delta S_{total}|} \times 100\% \tag{18}$$

$$I_{ha} = \frac{\Delta S_{ha}}{|\Delta S_{total}|} \times 100\% \tag{19}$$

Where ΔS_{total} is the total change in an ecological drought characteristic (e.g., $D_{dur}(i)$ and $D_{def}(i)$), and $|\Delta S_{total}|$ is the absolute value; ΔS_{cv} and ΔS_{ha} represent the changes of ecological drought characteristics due to climate variability and human activities, respectively; $S_{1,obs}$, and $S_{1,sim}$ denote ecological drought characteristics for the observed and simulated series during the undisturbed period, respectively; $S_{2,obs}$ and $S_{2,sim}$ denote ecological drought characteristics for the observed and simulated series during disturbed period, respectively; and I_{ha} and I_{cv} are the relative impacts of human activities and climate variability on ecological drought, respectively.

Table 2
Trend and change point analysis results for the annual precipitation and streamflow series for the XY and HX stations in the WRB.

Stations	MMK trend test (Z values)		Heuristic segmentation (year of change point)	
	Precipitation	Streamflow	Precipitation	Streamflow
XY	–1.58↓	**–5.09***↓	—	1990
HX	–1.33↓	**–5.22***↓	—	1990

Note: * in bold denotes significance at the 95 % confidence level. '↑' and '↓' indicate upward and downward trends, respectively.

4. Results

4.1. Reconstruction of natural streamflow

Trend analysis results using MMK method (listed in Table 2) showed that annual precipitation of the XY and HX stations showed a downward trend but not reached a significant level ($\alpha > 0.05$). However, the annual streamflow series of both stations showed a significant downward trend ($\alpha < 0.05$). To further explore hydrological variations in the WRB, the heuristic segmentation method was applied to investigate the change points in precipitation and streamflow series. The results (Table 2) showed that, for XY and HX stations, annual precipitation series had no significant change point while the annual streamflow series had a significant change point. The most significant change points ($\alpha < 0.05$) for both the XY and HX stations occurred in 1990.

In addition, Fig. 3 shows the DCCs of annual precipitation and streamflow for the XY and HX stations, indicating that the linear relationships between cumulated precipitation and streamflow at the two stations changed around 1990. Together, these variation analyses indicate that in addition to climate variability (e.g., precipitation), human activities may be another factor to cause the decrease of streamflow in the WRB. Based on the change point in 1990, we divided the entire study into two periods, i.e., undisturbed period (1961–1990) and disturbed period (1991–2017).

According to the above-mentioned division results for the study period, the observed meteorological and streamflow data during the undisturbed period (1961–1990) were used for the calibration and validation of the VIC model (Fig. 4). The warm-up period was 1961, 1962–1980 and 1981–1990 were the calibration and validation period, respectively. Thereafter, the observed meteorological data during the disturbed period (1991–2017) were used as input data to simulate the natural streamflow series of the XY and HX stations for the same period based on the calibrated VIC model. Table 3 shows that the evaluation criterion values, i.e., objective function (f), KGE, and $BIAS$ were 0.66, 0.80, –6.70 %, and 0.81, 0.84, 7.30 % for the XY station during the calibration and validation periods, respectively. These values for the HX station were 0.68, 0.81, and –0.90 % for the calibration period and 0.85, 0.89, and 4.80 % for the validation period, respectively. This shows that simulation results of the VIC model in the undisturbed period are accurate and reasonable to support the reconstruction of the natural streamflow series during the disturbed period.

4.2. The most suitable ecological flow

Fig. 5 shows the MSES identification process at the HX station using the nonparametric KDE function. The streamflow value corresponding to the maximum kernel density was selected as the MSES for each month to consider the seasonal patterns, and these values were then composed to a monthly variable threshold level. For the XY station, the maximum kernel density over 12 months ranged from 0.0014 to 0.0134, and the MSES values of different months ranged from 31.0 –212.7 m^3/s. For the HX station, the maximum kernel density and the corresponding MSES over the 12 months ranged from 0.0003 to 0.0037 and 42.3–368.1 m^3/s, respectively.

Fig. 6 shows a comparison of the monthly MSES series calculated via KDE method with those calculated by the Tennant and Smakhtin methods. Firstly, the MSES series calculated by the KDE method had the highest correlation coefficient (CC) with those calculated by Smakhtin (Q_{50} of the streamflow series) method, with the CC reaching 0.984 and 0.991 for XY and HX stations, respectively. While the KDE method and Tennant (60 % of the mean monthly streamflow) methods showed a correlation of 0.959 and 0.973 for XY and HX stations, respectively. Furthermore, twelve-month average values of the KDE, Tennant, and Smakhtin methods were 102.69, 92.04, 124,61 m^3/s for XY station, and

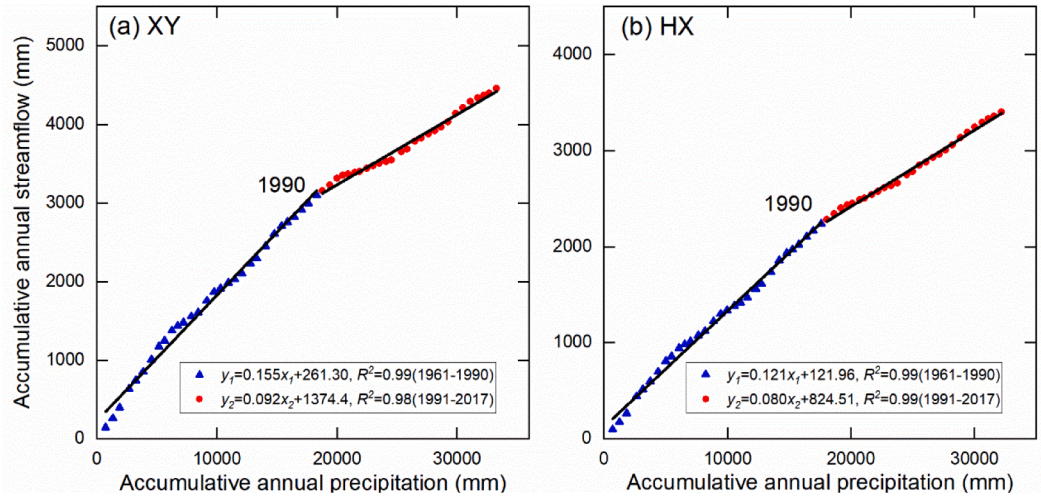

Fig. 3. Double cumulative curves of annual precipitation and streamflow for the XY (a) and HX (b) stations in the WRB.

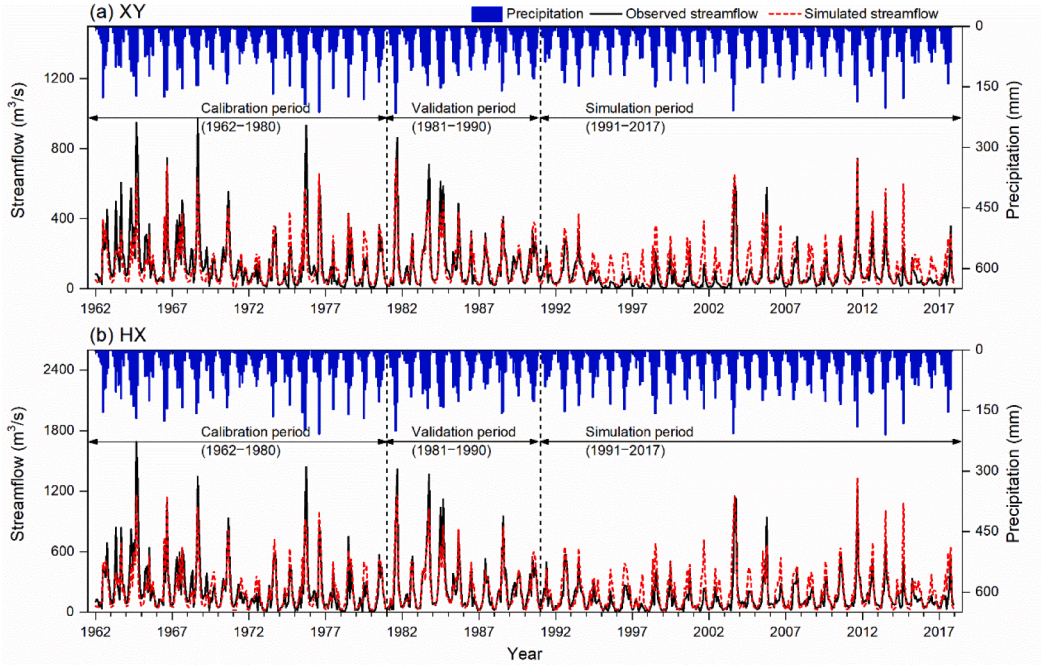

Fig. 4. Observed and simulated monthly streamflow series at the XY (a) and HX (b) stations during the calibration (1962–1980), validation (1981–1990), and simulation (1991–2017) periods.

Table 3
Performance of streamflow simulation for the XY and HX stations using the VIC model.

Station	Periods	Criterion values		
		$f = \max(NSE + \log NSE)$	*KGE*	*BIAS* (%)
XY	Calibration (1962–1980)	0.66	0.80	–6.70
	Validation (1981–1990)	0.81	0.84	7.30
HX	Calibration (1962–1980)	0.68	0.81	–0.90
	Validation (1981–1990)	0.85	0.89	4.80

165.91, 149.89, 209.33 m^3/s for HX station, respectively. The calculated values by the KDE method were mostly distributed between the values calculated by the Tennant and Smakhtin methods. Finally, the results of all the three methods showed consistent seasonal patterns, i.e., the largest monthly ecological streamflow occurs in September, and the smallest monthly ecological streamflow occurs in January, indicating that the MSES series calculated via KDE method is reasonable and can be used to determine whether a river ecosystem is under ecological drought conditions.

4.3. Identification of ecological drought

Fig. 7 shows the identified ecological drought events for the observed and simulated streamflow series at the XY and HX stations during the disturbed period (1991–2017). For the observed series (as shown in Fig. 7(a) and (d)) which is influenced by both climate variability and human activities, several long-term ecological drought events occurred, such as the multi-year drought events during 1995–1998 (35 months for the XY station and 34 months for the HX station), 1999–2003 (34 and 29 months for the XY and HX stations, respectively), and 2015–2017 (23 and 17 months for the XY and HX stations, respectively). For the

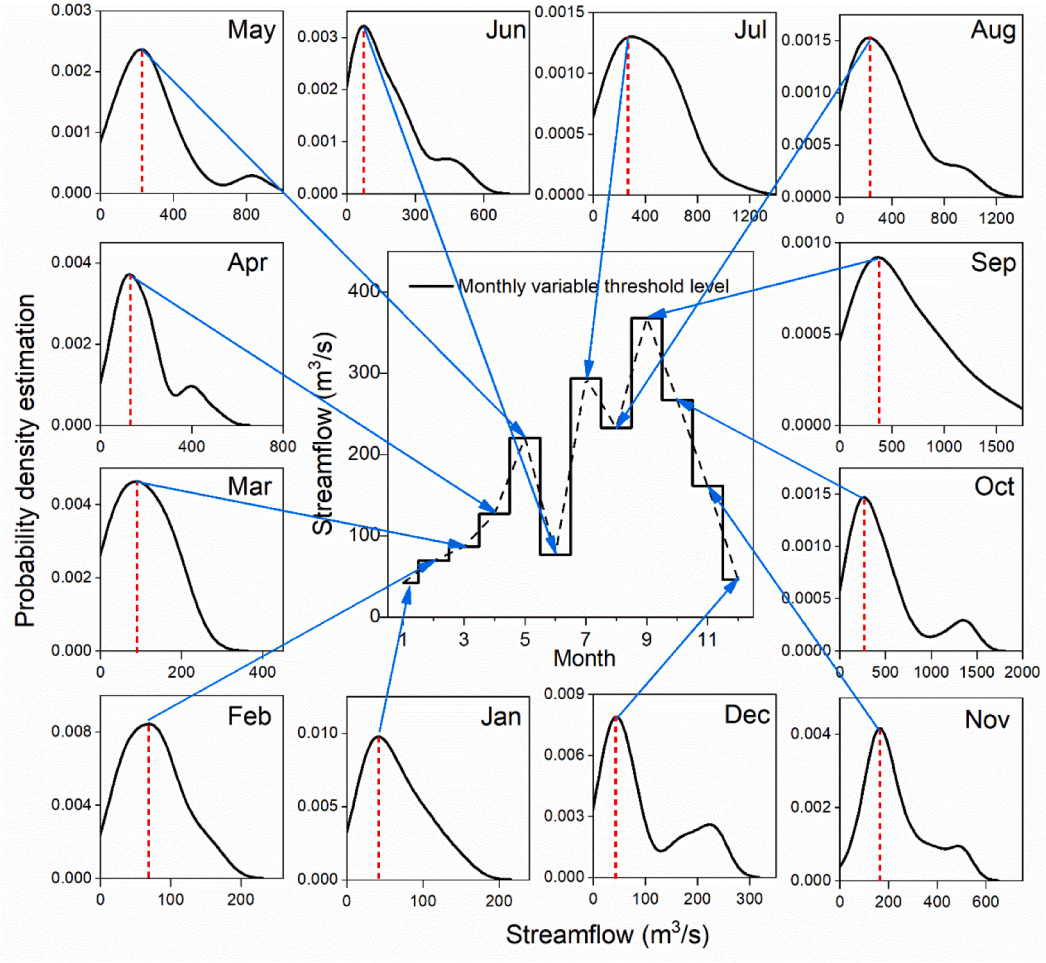

Fig. 5. Derivation of the monthly most suitable ecological streamflow from KDE curves of each month to compose the variable threshold level series for the HX station.

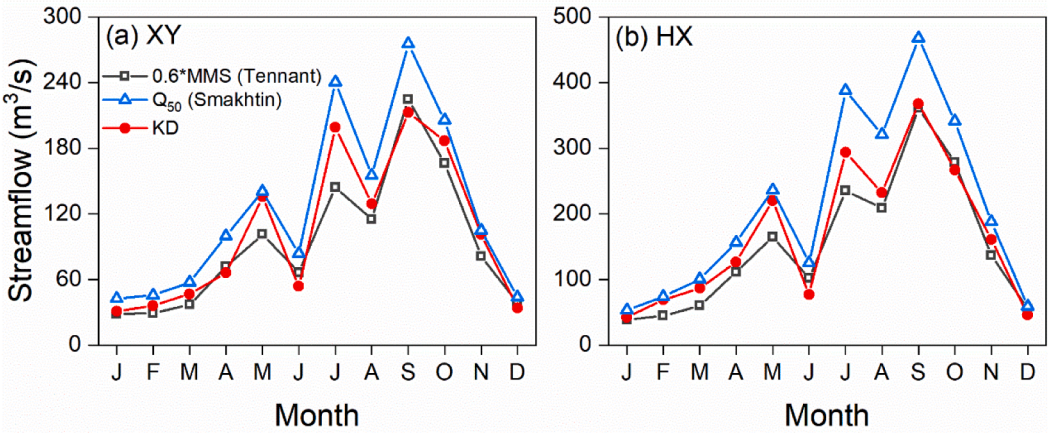

Fig. 6. Comparison of the monthly MSES calculated via KDE with those calculated using the Tennant method (0.6*MMS means 60% of the mean monthly streamflow) and the Smakhtin method (Q_{50} means the streamflow exceeded 50% of the period of record) for the XY (a) and HX (b) stations.

simulated series (Fig. 7(b) and (e)) which is influenced by only climate variability, some long-term drought events also occurred during the disturbed period, for example, the ecological drought in 1996–1998 (20 and 15 months for the XY and HX stations, respectively), 2001–2003 (14 and 16 months, respectively), and 2015–2017 (20 and 17 months, respectively). However, the drought durations of the long-term ecological drought events identified in simulated series are shorter than those identified in observed series on average, revealing that human activities led to the aggravation of duration of ecological drought in the WRB.

More intuitively, Fig. 7(c) and (f) compare the ecological drought deficit volumes of the simulated series with those of observed series. For the observed streamflow series at the XY station (Fig. 7(c)), the average deficit volumes for each ecological drought were 857.1 m^3/s in the 1990 s, 845.3 m^3/s in the 2000 s, and 363.3 m^3/s in the 2010 s, respectively.

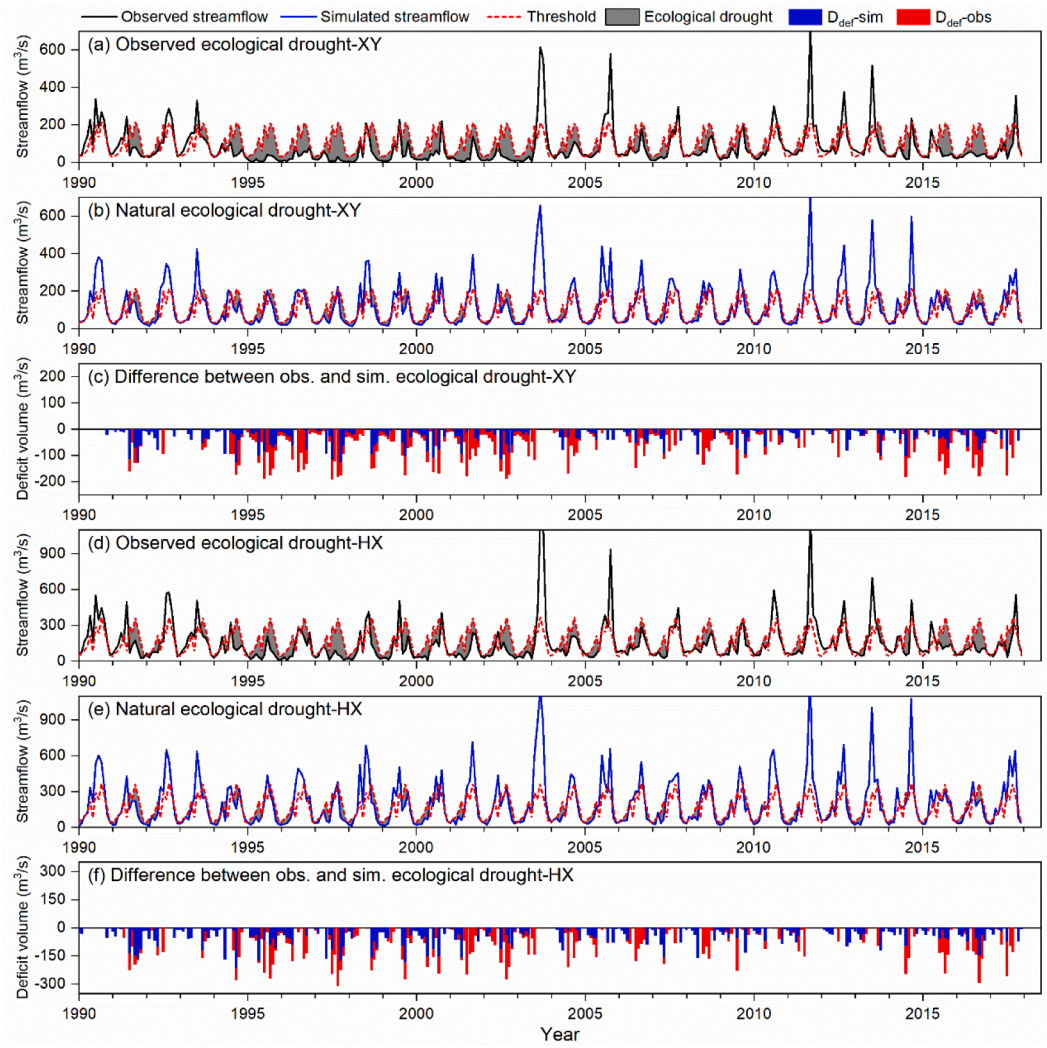

Fig. 7. Identification of ecological drought events for the observed and simulated series at the XY and HX stations during the disturbed period (1991–2017), and their ecological drought deficit volumes.

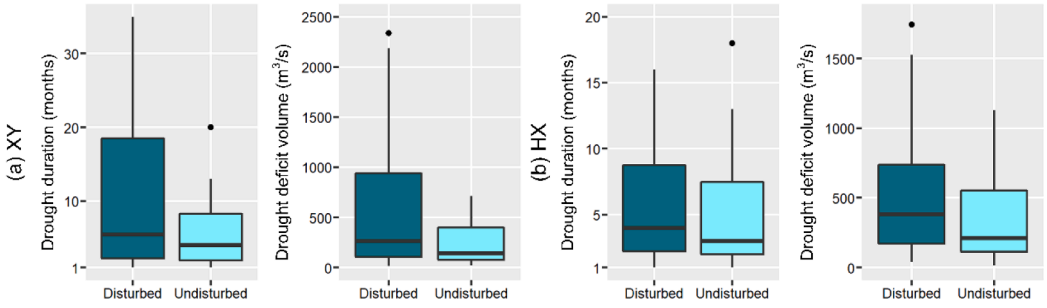

Fig. 8. Boxplots of ecological drought duration and deficit volumes of the observed streamflow series during the undisturbed (1961–1990) and disturbed (1991–2017) periods for the XY (a) and HX (b) stations.

These values for the HX station (Fig. 7(f)) were 659.2 m^3/s, 724.0 m^3/s, and 280.4 m^3/s in the 1990 s, 2000 s, and 2010 s, respectively. This indicated that under jointed influences of climate and human activities, the ecological drought in the 2000 s was the most serious, followed by those of the 1990 s and 2010 s. For the simulated series, the average deficit volumes of each ecological drought during the 1990 s, 2000 s, and 2010 s were 270.8, 161.6, and 133.4 m^3/s for the XY station and 352.2, 248.4, and 161.2 m^3/s for the HX station, respectively. These results revealed that under the impact of only climate variability, the severity of ecological drought gradually decreased from the 1990 s to the 2010 s. However, the deficit volumes of the ecological drought events identified in simulated series are lower than those identified in observed series on average, revealing that human activities led to the aggravation of deficit volumes of ecological drought in the WRB.

Fig. 8 shows a comparison of the ecological drought duration and deficit volumes of the observed streamflow series in the undisturbed and disturbed periods. For the XY station, the boxplots (Fig. 8(a)) show that both the median and upper quartile values of the drought duration (5.5

Table 4
Separating the effects of climate variability and human activities on ecological drought.

Station	ΔS_{total} (m^3/s)	ΔS_{cv} (m^3/s)	ΔS_{ha} (m^3/s)	I_{cv} (%)	I_{ha} (%)
XY	377.5	96.6	280.9	25.6 %	74.4 %
HX	249.8	106.6	143.3	42.7 %	57.3 %

and 18.5 months) and deficit volume (264.6 and 939.8 m^3/s) during the disturbed period were greater than those during the undisturbed period (4 and 8.25 months, and 144.2 and 398.2 m^3/s). Similarly, the median and upper quartile values of drought duration at the HX station (Fig. 8 (b)) were, respectively, 4 and 8.75 months for the disturbed period and 3 and 7.5 months for the undisturbed period; these values for drought deficit volume at the HX station were 381.8 and 739.6 m^3/s for the disturbed period and 210.1 and 551.3 m^3/s for the undisturbed period, respectively. Overall, ecological droughts in the disturbed period became more severe than those in the undisturbed period owing to the impacts of climate variability and human activities.

4.4. Quantification of the impacts of climate variability and human activities on ecological drought

Table 4 shows that the increases of ecological drought deficit volumes for the XY and HX stations were 377.5 and 249.8 m^3/s, respectively. Furthermore, the quantitative results based on the attribution framework in section 3.6 showed that, for XY station, climate change and human activities caused ecological drought deficit volumes to increase by 96.6 and 280.9 m3/s, respectively, and their contribution rates to the changes of ecological drought deficit volumes were 25.6 % and 74.4 %, respectively. For HX station, the increase of ecological drought deficit volumes due to climate change and human activities were 106.6 and 143.3 m3/s, respectively, and the contribution rates to the changes of ecological drought deficit volumes were 42.7 % and 57.3 %, respectively. Overall, human activities were the dominant factor for the aggravation of ecological drought (e.g., increased ecological drought deficit volumes) during the disturbed period (1991–2017) in the WRB.

5. Discussion

5.1. Rationality analysis of the most suitable ecological streamflow

In this study, we adopted the nonparametric KDE function to estimate probability density of the monthly streamflow series and then selected the streamflow values corresponding to the maximum probability density as the MSES for each month. In addition to the comparison with the two empirical methods, i.e., the Tennant and Smakhtin methods, we further compared the MSES calculated in the present study with the suitable ecological streamflow, considering the major economic fish and benthic species in other studies. Xin and Zhao (2008) pointed out that to better protect the ecological environment of the WRB, the ecological streamflow of the XY and HX stations should be>41.0 and 61.8 m^3/s, respectively. Ma and Su (2013) applied the RVA method to calculate the suitable river ecological streamflow as 36.7 and 75.8 m^3/s for XY and HX stations, respectively. The MSES values calculated using the KDE method were 31–66.4 m^3/s and 42.3–126.8 m^3/s during the low-flow periods (from November to April) at the XY and HX stations. This indicates that the MSES results calculated using the KDE in this study has a reasonable consideration of the living conditions of aquatic species.

5.2. Impacts of climate variability and human activities on ecological drought

The quantification results revealed that human activities are the dominant factor aggravating ecological drought in rivers in the WRB, with contribution rates of human influence to the increased ecological drought deficit volumes reaching 74.4 % and 57.3 % for XY and HX stations, respectively. These findings are similar with those of other studies over the WRB (Ren et al., 2016; Huang et al., 2017; Zou et al., 2018). For example, Ren et al. (2016) quantitatively separated the contributions of climate change and human activities to the reduction of streamflow in the WRB. The results showed that the decrease of streamflow caused by human activities at Xianyang and Huaxian stations were 1.610 billion m^3 and 2.310 billion m^3, respectively, with contributions to total streamflow decline reaching 66.7 % and 71.0 %, respectively. Zou et al. (2018) found that on shorter time scales (i.e., 3-month), the impacts of human activities on the aggravation of hydrological drought at Huaxian station were larger than those of climate change in spring, autumn, and winter, with the relative contribution rates reaching 59 %, 59 %, and 51 %, respectively.

Specifically, the direct human water abstraction for agricultural irrigation and industrial uses has caused a reduction in river streamflow in the WRB, thus aggravating ecological drought. Since the reform and opening up of China, the irrigation area in the WRB has continued to increase and reached 9500 km^2 in 2015 (Huang et al., 2016). The population of the basin increased from 22.04 million in 2000 to 24.62 million in 2010 (Xiong et al., 2018). The gross domestic product of the basin increased from 40.6 billion in 1990 to 2189.8 billion in 2017 (Ren et al., 2016). The average annual water consumption of the national economy in the basin reached 4.262 billion m^3 after the 1990 s, which was 52.6 % higher than that in the 1990 s (Huang et al., 2016). Overall, the increase in agricultural irrigation area and population, and the rapid economic development during the disturbed period of the WRB consumed more surface water resources, resulting in a sharp decrease in river streamflow and frequent ecological droughts, which had a serious impact on river ecosystems.

In addition, other human activities, such as returning farmland to forests, and soil and water conservation projects indirectly led to the reduction of river streamflow and the aggravation of ecological drought. The soil water conservation area in the WRB has increased from 15624 km^2 in 1990 to 33344 km^2 in 2006 (Zhang et al., 2021). After the implementation of the policy of returning farmland to forest in 1999, 5000 km^2 of farmland in Shaanxi Province was converted into forest land or grassland in 2003 (Zhao et al., 2017). Large-scale water and soil conservation projects in the WRB promoted precipitation interception and reduced land surface runoff, which eventually led to the reduction of river streamflow.

Fig. 9 shows a comparison of streamflow variations in the XY and HX stations during the undisturbed and disturbed periods. Results showed that the percentage decrease in streamflow in winter (from December to February) for the XY station ranged from 40 to 50 %, while that for the HX station was<25 %, indicating that human influence on the streamflow series were greater for the XY station than for the HX station. This period (December–February) is also the most prone season for ecological drought, which explains why the human influence on the ecological drought of the XY station is greater than that of the HX station.

Furthermore, climate variability also aggravates ecological drought in rivers through the hydrological cycle and then affects the river ecosystem in the WRB. For example, a decrease in precipitation reduces the recharge of river streamflow in the WRB (Xiong et al., 2018). An increase of temperature in WRB may cause an increase of evapotranspiration and in turn lead to a decrease of land surface runoff, thus reduces recharge to river streamflow (Liu et al., 2019).

Overall, due to the combined climatic and anthroponotic influence, the shortage of water resources in the WRB is becoming increasingly serious, resulting in ecological imbalance and environmental degradation. Xu et al. (2018) investigated the river ecosystem in the WRB during 2011–2013 and pointed out that the health of the river ecosystem in the WRB was poor. To solve these problems, the State Council of China approved the “key governance plan of the Weihe River Basin” and implemented a cross-basin water transfer project to extract the water of

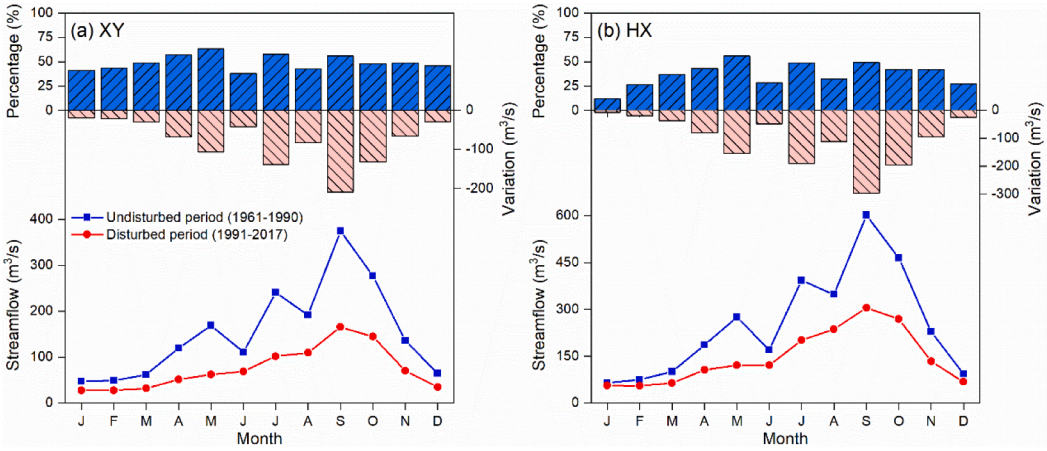

Fig. 9. Comparison of the observed mean monthly streamflow during the undisturbed and disturbed periods. Total streamflow variations (m^3/s) and their percentages (%) relative to the total streamflow during the undisturbed period for the XY (a) and HX (b) stations.

Hanjiang River to supplement the WRB in 2014. This project can directly provide 330 million m^3 water to the WRB annually. The proposed methods of the present study could provide reference methodology for similar studies in other regions of the world, and provide scientific guidance for the government's water diversion projects, thus aiding in alleviating the ecological drought in rivers and improving the carrying capacity of the river ecosystem in the WRB.

5.3. Uncertainty and limitations

Although the MSES calculation using the KDE function and the quantification framework based on hydrological simulation are suitable tools for analysing the effects of climate variability and human activities on ecological drought in rivers, some uncertainties and limitations in this study are still worth emphasizing.

When using the probability fitting method, the sample length affects the probability density estimation (Wang et al., 2021b). Therefore, when the KDE method is used in other regions, the length of the available sample data should be sufficient for probability fitting. In this study, a 30-year streamflow dataset from the undisturbed period (1961–1990) was used for probability density estimation, which meets the criterion of sample size recommended by the WMO (i.e., $\geq$ 30 years) and can be used as a reference sample to study the impact of climate variability. In addition, the aquatic ecosystem in a river is complex and diverse. Therefore, the identification and analysis of ecological drought in rivers and the attribution of its driving factors are usually complex and difficult. Although this study selected MSES as the threshold for identification of ecological drought, double- or multi-threshold methods can be considered in future research to better capture the ecological drought events (Park et al., 2020). Furthermore, because of the lack of data about ecosystem responses to streamflow alterations in the study area, we adopted the hydrological methods for MSES calculation. Therefore, future studies should focus on developing a consistent eco-hydrological monitoring and forecasting system that consider the response of the aquatic ecosystems to streamflow variations (Barnosky et al., 2012; Pastor et al., 2014).

In addition, the use of hydrological models usually bring uncertainty (Van Loon et al., 2013; Wang et al., 2020; Mohammadi et al., 2021, 2022; Rahman et al., 2022). Therefore, when carrying out ecological drought research based on hydrological models in other regions, one should carefully select the appropriate hydrological model and set appropriate objective functions to calibrate the models to ensure the accurate capture of the low-flow process as much as possible. This study selected 30 years of data in the undisturbed period (1961–1990) for model calibration and verification and then simulated 27 years of streamflow data in the disturbed period (1991–2017). The lengths of the two periods were similar with each other, and the objective function ensure the VIC model could capture both low and high flow processes well.

6. Conclusion

In this study, we adopted the KDE function to estimate the probability density of the monthly streamflow and selected streamflow values corresponding to the maximum density as the MSES to compose a variable threshold series for the identification of ecological drought. Subsequently, a quantification approach based on hydrological model simulation was proposed to separate the effects of climate variability and human activities on ecological drought. The basic requirements of the approach were the observed meteorological and streamflow data of the undisturbed period to calibrate/validate the hydrological model and the observed meteorological data of the disturbed period to simulate streamflow during the same period.

It is concluded that the streamflow of the Xixian and Huaxian stations within the WRB had a significant downward trend ($\alpha < 0.05$) and both change points of streamflow series of the two stations appeared in 1990. Besides, simulation results revealed that VIC model can accurately simulate streamflow process of the two stations during disturbed period (1961–1990), so as to support the reconstruction of the natural streamflow series during disturbed period (1991–2017). More importantly, the attribution analysis showed that the impacts of climate variability and human activities on the aggravation of ecological drought were 25.6 % and 74.4 % for the XY station, and 42.7 % and 57.3 % for the HX station, respectively, revealing that human activities were the dominant factor for the aggravation of ecological drought in the WRB after 1990.

Overall, the proposed integrated approach for comprehensive understanding and quantification of ecological drought in rivers provides water managers with suitable tools to explore how climate variability and human activities alter ecological drought. However, in this study, changes of land use and vegetation conditions are not considered in the simulation of VIC model. In the future studies, the dynamic changes of the underlying vegetation should be considered in the model simulation processes. More importantly, it will be more meaningful to further study the impacts of different meteorological flux changes (i.e., precipitation changes and temperature changes) and different types of anthropogenic water use behaviours (i.e., reservoir regulations and direct water abstraction) on ecological drought.

CRediT authorship contribution statement

Shanhu Jiang: Conceptualization, Writing – review & editing.

Menghao Wang: Writing – review & editing. **Liliang Ren:** Funding acquisition. **Yating Liu:** Methodology. **Le Zhou:** Methodology. **Hao Cui:** Methodology. **Chong-Yu Xu:** Writing – review & editing, Funding acquisition.

Declaration of Competing Interest

The authors declare that they have no known competing financial interests or personal relationships that could have appeared to influence the work reported in this paper.

Data availability

No data was used for the research described in the article.

Acknowledgments

This work was financially supported by the National Natural Science Foundation of China (U2243203, 51979069); the Fundamental Research Funds for the Central Universities (B200204029); the National Natural Science Foundation of Jiangsu Province, China (BK20211202); and the Research Council of Norway (FRINATEK Project 274310).

References

Akcura, M., Turan, V., Kokten, K., Kaplan, M., 2019. Fatty acid and some micro element compositions of cluster bean (Cyamopsis tetragonoloba) genotype seeds growing under Mediterranean climate. Ind. Crops Prod. 128, 140–146. https://doi.org/10.1016/j.indcrop.2018.10.062.

Apurv, T., Cai, X., 2020. Drought Propagation in Contiguous U.S. Watersheds: A Process-Based Understanding of the Role of Climate and Watershed Properties. Water Resour. Res. 56, 1–23. https://doi.org/10.1029/2020WR027755.

Barnosky, A.D., Hadly, E.A., Bascompte, J., Berlow, E.L., Brown, J.H., Fortelius, M., Getz, W.M., Harte, J., Hastings, A., Marquet, P.A., Martinez, N.D., Mooers, A., Roopnarine, P., Vermeij, G., Williams, J.W., Gillespie, R., Kitzes, J., Marshall, C., Matzke, N., Mindell, D.P., Revilla, E., Smith, A.B., 2012. Approaching a state shift in Earth's biosphere. Nature 486, 52–58. https://doi.org/10.1038/nature11018.

Bernaola-Galván, P., Ivanov, P.C., Nunes Amaral, L.A., Stanley, H.E., 2001. Scale invariance in the nonstationarity of human heart rate. Phys. Rev. Lett. 87, 1–4. https://doi.org/10.1103/PhysRevLett.87.168105.

S. Bilen V. Turan Enzymatic Analyses in Soils N. Amaresan P. Patel D. Amin Practical Handbook on Agricultural Microbiology. Springer Protocols Handbooks 2022 Humana New York, NY 10.1007/978-1-0716-1724-3_50.

Bowman, A.W., Azzalini, A., 1997. Applied Smoothing Techniques for Data Analysis: The Kernel Approach with S-Plus Illustrations. 18. OUP Oxford.

Carlson, T.N., Gillies, R.R., Perry, E.M., 1994. A method to make use of thermal infrared temperature and NDVI measurements to infer surface soil water content and fractional vegetation cover. Remote Sens. Rev. 9, 161–173. https://doi.org/10.1080/02757259409532220.

Crausbay, S.D., Ramirez, A.R., Carter, S.L., Cross, M.S., Hall, K.R., Bathke, D.J., Betancourt, J.L., Colt, S., Cravens, A.E., Dalton, M.S., Dunham, J.B., Hay, L.E., Hayes, M.J., McEvoy, J., McNutt, C.A., Moritz, M.A., Nislow, K.H., Raheem, N., Sanford, T., 2017. Defining ecological drought for the twenty-first century. Bull. Am. Meteorol. Soc. 98, 2543–2550. https://doi.org/10.1175/BAMS-D-16-0292.1.

Duan, Q., Sorooshian, S., Gupta, V., 1992. Effective and Efficient Global Optimization. Water Resour. Res. 28, 1015–1031.

Eltahir, E.A.B., Yeh, P.J.F., 1999. On the asymmetric response of aquifer water level to floods and droughts in Illinois. Water Resour. Res. 35, 1199–1217. https://doi.org/10.1029/1998WR900071.

Fang, W., Huang, S., Huang, Q., Huang, G., Wang, H., Leng, G., Wang, L., 2020. Identifying drought propagation by simultaneously considering linear and nonlinear dependence in the Wei River basin of the Loess Plateau. China. J. Hydrol. 591, 125287 https://doi.org/10.1016/j.jhydrol.2020.125287.

Gai, L., Nunes, J.P., Baartman, J.E.M., Zhang, H., Wang, F., de Roo, A., Ritsema, C.J., Geissen, V., 2019. Assessing the impact of human interventions on floods and low flows in the Wei River Basin in China using the LISFLOOD model. Sci. Total Environ. 653, 1077–1094. https://doi.org/10.1016/j.scitotenv.2018.10.379.

Ghasempour, R., Roushangar, K., Kirca, V.S.O., Demirel, M.C., 2022. Analysis of spatiotemporal variations of drought and its correlations with remote sensing-based indices via wavelet analysis and clustering methods. Hydrol. Res. 53 (1), 175–192.

Gou, J., Miao, C., Duan, Q., Tang, Q., Di, Z., Liao, W., Wu, J., Zhou, R., 2020. Sensitivity Analysis-Based Automatic Parameter Calibration of the VIC Model for Streamflow Simulations Over China. Water Resour. Res. 56, 1–19. https://doi.org/10.1029/2019WR025968.

Gudmundsson, L., Boulange, J., Do, H.X., et al., 2021. Globally observed trends in mean and extreme river flow attributed to climate change. Science 371 (6534), 1159–1162.

Hamed, K.H., Ramachandra Rao, A., 1998. A modified Mann-Kendall trend test for autocorrelated data. J. Hydrol. 204, 182–196. https://doi.org/10.1016/S0022-1694(97)00125-X.

M. Hasanuzzaman M. Fujita H. Oku M.T. Islam Plant Tolerance to Environmental Stress: Role of Phytoprotectants (1st ed.). 2019 CRC Press 10.1201/9780203705315.

Huang, S., Chang, J., Huang, Q., Chen, Y., Leng, G., 2016. Quantifying the relative contribution of climate and human impacts on runoff change based on the budyko hypothesis and SVM model. Water Resour. Manag. 30, 2377–2390. https://doi.org/10.1007/s11269-016-1286-x.

Huang, S., Huang, Q., Leng, G., Zhao, M., Meng, E., 2017. Variations in annual water-energy balance and their correlations with vegetation and soil moisture dynamics: A case study in the Wei River Basin. China. J. Hydrol. 546, 515–525. https://doi.org/10.1016/j.jhydrol.2016.12.060.

Jiang, S., Ren, L., Yong, B., Singh, V.P., Yang, X.L., Yuan, F., 2011. Quantifying the effects of climate variability and human activities on runoff from the Laohahe basin in northern China using three different methods. Hydrol. Process. 25, 2492–2505.

Jiang, T., Su, X., Singh, V.P., Zhang, G., 2021b. A novel index for ecological drought monitoring based on ecological water deficit. Ecol. Ind. 129 https://doi.org/10.1016/j.ecolind.2021.107804.

Jiang, S., Wang, M., Ren, L., Xu, C.Y., Yuan, F., Liu, Y., Lu, Y., Shen, H., 2019. A framework for quantifying the impacts of climate change and human activities on hydrological drought in a semiarid basin of Northern China. Hydrol. Process. 33, 1075–1088. https://doi.org/10.1002/hyp.13386.

Jiang, S., Wei, L., Ren, L., Xu, C.Y., Zhong, F., Wang, M., Zhang, L., Yuan, F., Liu, Y., 2021a. Utility of integrated IMERG precipitation and GLEAM potential evapotranspiration products for drought monitoring over mainland China. Atmos. Res. 247, 105141 https://doi.org/10.1016/j.atmosres.2020.105141.

Jiang, S., Zhou, L., Ren, L., Wang, M., Xu, C.Y., Yuan, F., Liu, Y., Yang, X., Ding, Y., 2021c. Development of a comprehensive framework for quantifying the impacts of climate change and human activities on river hydrological health variation. J. Hydrol. 600 https://doi.org/10.1016/j.jhydrol.2021.126566.

Kim, J.S., Jain, S., Lee, J.H., Chen, H., Park, S.Y., 2019. Quantitative vulnerability assessment of water quality to extreme drought in a changing climate. Ecol. Ind. 103, 688–697. https://doi.org/10.1016/j.ecolind.2019.04.052.

Liang, X., Lettenmaier, D.P., Wood, E.F., Burges, S.J., 1994. A simple hydrologically based model of land surface water and energy fluxes for GSMs. J. Geophys. Res. [Atmos.] 99 (D7), 14415–14428.

Liu, S., Huang, S., Xie, Y., Huang, Q., Wang, H., Leng, G., 2019. Assessing the non-stationarity of low flows and their scale-dependent relationships with climate and human forcing. Sci. Total Environ. 687, 244–256. https://doi.org/10.1016/j.scitotenv.2019.06.025.

Ma, L., Huang, Q., Huang, S.Z., Liu, D.P., Leng, G.Y., Wang, L., Li, P., 2022. Propagation dynamics and causes of hydrological drought in response to meteorological drought at seasonal timescales. Hydrol. Res. 53 (1), 193–205.

Ma, D., Luo, W., Yang, G., Lu, J., Fan, Y., 2019. A study on a river health assessment method based on ecological flow. Ecol. Model. 401, 144–154. https://doi.org/10.1016/j.ecolmodel.2018.11.023.

Ma, X., Su, X., 2013. Research on the eco-environment water requirements and its satisfaction of the middle and downstream of Weihe River based on RVA. Agric. Res. in the Arid Areas. 31 (6), 220–224 (in Chinese).

McEvoy, J., Bathke, D.J., Burkardt, N., Cravens, A.E., Haigh, T., Hall, K.R., Hayes, M.J., Jedd, T., Podèbradská, M., Wickham, E., 2018. Ecological drought: Accounting for the non-human impacts of water shortage in the upper Missouri Headwaters Basin, Montana, USA. Resources 7. https://doi.org/10.3390/resources7010014.

McManamay, R.A., Orth, D.J., Dolloff, C.A., Mathews, D.C., 2013. Application of the ELOHA framework to regulated rivers in the upper tennessee river basin: A case study. Environ. Manage. 51, 1210–1235. https://doi.org/10.1007/s00267-013-0055-3.

McMillan, H.K., 2021. A review of hydrologic signatures and their applications. Wiley Interdiscip. Rev. Water 8, 1–23. https://doi.org/10.1002/wat2.1499.

Measho, S., Chen, B., Trisurat, Y., Pellikka, P., Guo, L., Arunyawat, S., Tuankrua, V., Ogbazghi, W., Yemane, T., 2019. Spatio-temporal analysis of vegetation dynamics as a response to climate variability and drought patterns in the Semiarid Region. Eritrea. Remote Sens. 11 https://doi.org/10.3390/RS11060724.

Mishra, A.K., Singh, V.P., 2010. A review of drought concepts. J. Hydrol. 391, 202–216. https://doi.org/10.1016/j.jhydrol.2010.07.012.

Mohammadi, B., 2022. OPEN IHACRES, GR4J and MISD - based multi conceptual - machine learning approach for rainfall - runoff modeling. Sci. Rep. 1–21 https://doi.org/10.1038/s41598-022-16215-1.

Mohammadi, B., Moazenzadeh, R., Christian, K., Duan, Z., 2021. Improving streamflow simulation by combining hydrological process-driven and artificial intelligence-based models. Environ. Sci. Pollut. Res. 28, 65752–65768. https://doi.org/10.1007/s11356-021-15563-1.

Nanzad, L., Zhang, J., Tuvdendorj, B., Nabil, M., Zhang, S., Bai, Y., 2019. NDVI anomaly for drought monitoring and its correlation with climate factors over Mongolia from 2000 to 2016. J. Arid Environ. 164, 69–77. https://doi.org/10.1016/j.jaridenv.2019.01.019.

Oudin, L., Andréassian, V., Mathevet, T., Perrin, C., Michel, C., 2006. Dynamic averaging of rainfall-runoff model simulations from complementary model parameterizations. Water Resour. Res. 42, 1–10. https://doi.org/10.1029/2005WR004636.

Ow, L.F., Whitehead, D., Walcroft, A.S., Turnbull, M.H., 2010. Seasonal variation in foliar carbon exchange in Pinus radiata and Populus deltoides: Respiration acclimates fully to changes in temperature but photosynthesis does not. Glob. Chang. Biol. 16, 288–302. https://doi.org/10.1111/j.1365-2486.2009.01892.x.

Palmer, M., Ruhi, A., 2019. Linkages between flow regime, biota, and ecosystem processes: Implications for river restoration. Science 365 (6459). https://doi.org/10.1126/science.aaw2087.

Park, S.Y., Sur, C., Lee, J.H., Kim, J.S., 2020. Ecological drought monitoring through fish habitat-based flow assessment in the Gam river basin of Korea. Ecol. Ind. 109, 105830 https://doi.org/10.1016/j.ecolind.2019.105830.

Pastor, A.V., Ludwig, F., Biemans, H., Hoff, H., Kabat, P., 2014. Accounting for environmental flow requirements in global water assessments. Hydrol. Earth Syst. Sci. 18, 5041–5059. https://doi.org/10.5194/hess-18-5041-2014.

Peters, E., Torfs, P.J.J.F., van Lanen, H.A.J., Bier, G., 2003. Propagation of drought through groundwater - A new approach using linear reservoir theory. Hydrol. Process. 17, 3023–3040. https://doi.org/10.1002/hyp.1274.

Poff, N.L., Richter, B.D., Arthington, A.H., Bunn, S.E., Naiman, R.J., Kendy, E., Acreman, M., Apse, C., Bledsoe, B.P., Freeman, M.C., Henriksen, J., Jacobson, R.B., Kennen, J.G., Merritt, D.M., O'Keeffe, J.H., Olden, J.D., Rogers, K., Tharme, R.E., Warner, A., 2010. The ecological limits of hydrologic alteration (ELOHA): A new framework for developing regional environmental flow standards. Freshw. Biol. 55, 147–170. https://doi.org/10.1111/j.1365-2427.2009.02204.x.

Rahman, K.U., Pham, Q.B., Jadoon, K.Z., Shahid, M., Kushwaha, D.P., Duan, Z., Mohammadi, B., Khedher, K.M., Anh, D.T., 2022. Comparison of machine learning and process-based SWAT model in simulating streamflow in the Upper Indus Basin. Appl. Water Sci. 12, 1–19. https://doi.org/10.1007/s13201-022-01692-6.

Ren, L., Shen, H., Yuan, F., Zhao, C., Yang, X., Zheng, P., 2016. Hydrological drought characteristics in the Weihe catchment in a changing environment. Adv. Water Sci. 27(4), 492–500. 10.14042/j.cnki.32.1309.2016.04.002. (in Chinese).

Richter, B.D., Warner, A.T., Meyer, J.L., Lutz, K., 2006. A collaborative and adaptive process for developing environmental flow recommendations. River Res. Appl. 22, 297–318. https://doi.org/10.1002/rra.892.

Roodposhti, M.S., Safarrad, T., Shahabi, H., 2017. Drought sensitivity mapping using two one-class support vector machine algorithms. Atmos. Res. 193, 73–82. https://doi.org/10.1016/j.atmosres.2017.04.017.

Shafroth, P.B., Wilcox, A.C., Lytle, D.A., Hickey, J.T., Andersen, D.C., Beauchamp, V.B., Hautzinger, A., McMullen, L.E., Warner, A., 2010. Ecosystem effects of environmental flows: Modelling and experimental floods in a dryland river. Freshw. Biol. 55, 68–85. https://doi.org/10.1111/j.1365-2427.2009.02271.x.

Smakhtin, V., Revenga, C., Döll, P., 2004. A pilot global assessment of environmental water requirements and scarcity. Water Int. 29, 307–317. https://doi.org/10.1080/02508060408691785.

H.M. Tauqeer V. Turan M. Iqbal J.A. Malik Production of Safer Vegetables from Heavy Metals Contaminated Soils: The Current Situation, Concerns Associated with Human Health and Novel Management Strategies 2022 Advances in Bioremediation and Phytoremediation for Sustainable Soil Management. Springer Cham 10.1007/978-3-030-89984-4_19.

Tennant, D.L., 1976. Instream Flow Regimens for Fish, Wildlife, Recreation and Related Environmental Resources. Fisheries 1, 6–10. https://doi.org/10.1577/1548-8446(1976)001<0006:ifrffw>2.0.co;2.

Tharme, R.E., 2003. A global perspective on environmental flow assessment: Emerging trends in the development and application of environmental flow methodologies for rivers. River Res. Appl. 19, 397–441. https://doi.org/10.1002/rra.736.

Tonkin, J.D., Poff, N.L., Bond, N.R., et al., 2019. Prepare river ecosystems for an uncertain future. Nature 570 (7761), 301–303.

Van Loon, A.F., Gleeson, T., Clark, J., Van Dijk, A.I.J.M., Stahl, K., Hannaford, J., Di Baldassarre, G., Teuling, A.J., Tallaksen, L.M., Uijlenhoet, R., Hannah, D.M., Sheffield, J., Svoboda, M., Verbeiren, B., Wagener, T., Rangecroft, S., Wanders, N., Van Lanen, H.A.J., 2016. Drought in the Anthropocene. Nat. Geosci. 9, 89–91. https://doi.org/10.1038/ngeo2646.

Van Loon, A.F., Van Lanen, H.A.J., 2013. Making the distinction between water scarcity and drought using an observation-modeling framework. Water Resour. Res. 49, 1483–1502. https://doi.org/10.1002/wrcr.20147.

Vicente-Serrano, S.M., Quiring, S.M., Peña-Gallardo, M., Yuan, S., Domínguez-Castro, F., 2020. A review of environmental droughts: Increased risk under global warming? Earth-Science Rev. 201, 102953 https://doi.org/10.1016/j.earscirev.2019.102953.

Wanders, N., Wada, Y., 2015. Human and climate impacts on the 21st century hydrological drought. J. Hydrol. 526, 208–220. https://doi.org/10.1016/j.jhydrol.2014.10.047.

Wang, M., Jiang, S., Ren, L., Xu, C.Y., Yuan, F., Liu, Y., Yang, X., 2020. An approach for identification and quantification of hydrological drought termination characteristics of natural and human-influenced series. J. Hydrol. 590 https://doi.org/10.1016/j.jhydrol.2020.125384.

Wang, M., Jiang, S., Ren, L., Xu, C.Y., Menzel, L., Yuan, F., Xu, Q., Liu, Y., Yang, X., 2021a. Separating the effects of climate change and human activities on drought propagation via a natural and human-impacted catchment comparison method. J. Hydrol. 603, 126913 https://doi.org/10.1016/j.jhydrol.2021.126913.

Wang, M., Jiang, S., Ren, L., Xu, C.Y., Wei, L., Cui, H., Yuan, F., Liu, Y., Yang, X., 2022. The Development of a Nonstationary Standardised Streamflow Index Using Climate and Reservoir Indices as Covariates. Water Resour. Manag. 36, 1377–1392. https://doi.org/10.1007/s11269-022-03088-2.

Wang, W., Wang, J., Romanowicz, R., 2021b. Uncertainty in SPI calculation and its impact on drought assessment in different climate regions over China. J. Hydrometeorol. 22, 1369–1383. https://doi.org/10.1175/JHM-D-20-0256.1.

Wilson, R.S., Franklin, C.E., 2002. Testing the beneficial acclimation hypothesis. Trends Ecol. Evol. 17, 66–70.

Xin, C., Zhao, W., 2008. Calculation of ecological base flow in the middle and lower reaches of the Weihe River. J. Water. Res. & Water Eng. 19 (3), 90–92 (in Chinese).

Xiong, L., Jiang, C., Du, T., 2014. Statistical attribution analysis of the nonstationarity of the annual runoff series of the Weihe River. Water Sci. Technol. 70, 939–946. https://doi.org/10.2166/wst.2014.322.

Xiong, B., Xiong, L., Chen, J., Xu, C.Y., Li, L., 2018. Multiple causes of nonstationarity in the Weihe annual low-flow series. Hydrol. Earth Syst. Sci. 22, 1525–1542. https://doi.org/10.5194/hess-22-1525-2018.

Xu, Z., Gu, X., Liu, L., 2018. Investigation and assessment on river health of Weihe River Basin. Water Resour. Prot. 34 (1), 1–7 (in Chinese).

Yan, H., Zhou, G., Yang, F., Lu, X., 2019. DEM correction to the TVDI method on drought monitoring in karst areas. Int. J. Remote Sens. 40, 2166–2189. https://doi.org/10.1080/01431161.2018.1500732.

Yevjevich, V.M. (1967). Objective approach to definitions and investigations of continental hydrologic droughts, An. Hydrol. Papers (Colorado State University). No. 23.

Yuan, F., Wang, B., Shi, C., Cui, W., Zhao, C., Liu, Y., Ren, L., Zhang, L., Zhu, Y., Chen, T., Jiang, S., Yang, X., 2018. Evaluation of hydrological utility of IMERG Final run V05 and TMPA 3B42V7 satellite precipitation products in the Yellow River source region, China. J. Hydrol. 567, 696–711. https://doi.org/10.1016/j.jhydrol.2018.06.045.

Zhang, T., Su, X., Feng, K., 2021. The development of a novel nonstationary meteorological and hydrological drought index using the climatic and anthropogenic indices as covariates. Sci. Total Environ. 786, 147385 https://doi.org/10.1016/j.scitotenv.2021.147385.

Zhao, A., Zhang, A., Lu, C., Wang, D., Wang, H., Liu, H., 2017. Spatiotemporal variation of vegetation coverage before and after implementation of Grain for Green Program in Loess Plateau, China. Ecol. Eng. 104, 13–22. https://doi.org/10.1016/j.ecoleng.2017.03.013.

Zhou, Y.L., Zhou, P., 2021. Decline in net primary productivity caused by severe droughts: evidence from the Pearl River basin in China. Hydrol. Res. 52 (6), 1559–1576.

Zou, L., Xia, J., She, D., 2018. Analysis of Impacts of Climate Change and Human Activities on Hydrological Drought: a Case Study in the Wei River Basin, China. Water Resour. Manag. 32, 1421–1438. https://doi.org/10.1007/s11269-017-1877-1.